6th European Conference on Computational Mechanics (ECCM 6)
7th European Conference on Computational Fluid Dynamics (ECFD 7)
11 – 15 June 2018, Glasgow, UK

COMPUTATIONAL EVALUATION OF BENDING FATIGUE TEST ON ELECTRODE OF LITHIUM-ION BATTERY

YOSHINAO KISHIMOTO[1], YUKIYOSHI KOBAYASHI[1], TOSHIHISA OHTSUKA[1], TATSUYA TSURUTA[1], KYOHEI NAKAMURA[1] AND YUKI TSUKAGOSHI[1]

[1]Department of Mechanical Engineering, Faculty of Engineering, Tokyo City University
1-28-1 Tamazutsumi, Setagaya-ku, Tokyo, Japan
ykishimo@tcu.ac.jp, http://www.tcu.ac.jp

Key words: Lithium-Ion Battery, Strength of Materials, Fatigue, Finite Element Method.

Abstract. This paper has proposed a fatigue testing method for the active material of the Lithium-ion battery (LIB) by applying the bending deformation repeatedly and investigated the mechanical property of the active material subjected to the cyclic load. The bending fatigue test was performed by using the anode sheet of the LIB that is graphite coated on copper foil. The finite element (FE) simulation was also performed to evaluate the proposed testing method. In the actual test, the crack initiation was observed at the graphite or the copper foil. The location of the crack initiation depended on the thicknesses of the graphite and the copper foil. At the first bending, the plastic deformation occurred in the copper foil. After that, the repeated variable strain occurred in the copper foil during the test. Then the maximum strain was equal to the strain under the bending, and the minimum strain was equal to the permanent strain. The mechanical behavior computed by the FE simulation agreed with that in the actual test. The strain of the graphite in the FE simulation was substituted for the actual value that is difficult to be measured directly. The strain amplitude of the graphite monotonically decreased against the number of cycles until the crack initiation.

1 INTRODUCTION

The application of the Lithium-ion battery (LIB) is expanded to electric automobiles. The reliability of the battery should be established to prevent serious incidents because of the high energy density. The cyclic load by the vibration and the thermal stress causes the fatigue damage of the electrode apart from the microscopic fatigue by the charge and discharge [1]. The electrode is the active material coated on the metallic foil. The strength and the stiffness of the active material are much lower than those of the metallic foil. Even though the active material has relatively low strength, some studies take the approach that the mechanical properties of the active material are ignored in the computational homogenization [2-9]. There has been little study done concerning the mechanical properties of the active material including the coating adhesion strength between the active material and the metallic foil [10].

This study has proposed a fatigue testing method for the active material by applying the bending deformation repeatedly in order to investigate the mechanical property of the active material subjected to the cyclic load. The bending fatigue test was performed by using the anode sheet of the LIB that is graphite coated on copper foil. The finite element (FE) simulation was also performed to evaluate the proposed testing method.

2 METHODS

2.1 Specimen

The two types of the specimens were prepared. The specimen A is just the metallic foil (pure copper, thickness: 0.1 or 0.3 mm) made of copper as shown in Fig. 1. The strain gauges were attached at the points A to H. The tensile strain along the longitudinal direction (the horizontal direction in the figure) was measured in the bending fatigue test. The specimen B is the anode sheet for the LIB as shown in Fig.2. Table 1 shows the constituent materials of the specimen. The specimen B was composed of the copper foil (thickness: 0.1 or 0.3 mm) coated with the graphite and the thermoplastic fluropolymer binder polyvinylidene fluoride (PVDF).

2.2 Bending fatigue testing machine

Figure 3 shows the bending fatigue testing machine developed in this study. The specimen was attached on the curved plate (curvature: 50 mm). The arm flapped, and the specimen was bended repeatedly during the motor rotated. The curvature of the specimen was controlled by the curved plate. In the fatigue test. The rotating speed of the motor was set to 5, 7 or 10 Hz. The camera was set above the specimen and the behavior of the specimen was observed. Then the crack initiation on the specimen was defined as the fatigue life of the specimen.

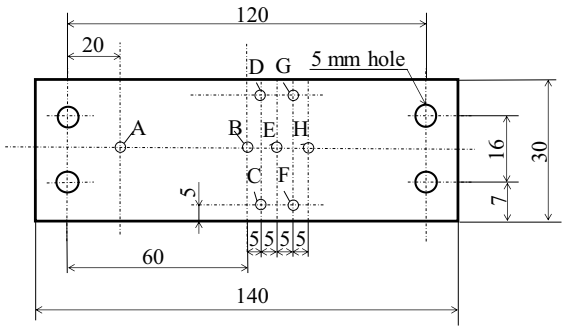

Figure 1: Shape of specimen A

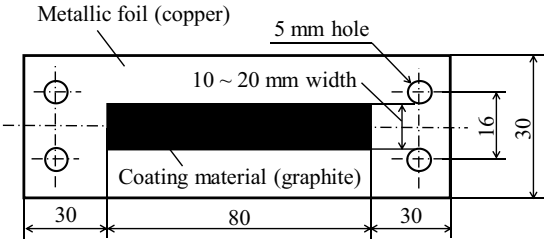

Figure 2: Shape of specimen B

Table 1: Constituent materials of specimens

Metallic foil	Material		Pure copper (C1100 in JIS, equivalent to C11000 in CDA)
	Thickness		0.1 mm or 0.3 mm
	Young's modulus		118 GPa
	Poisson's ratio		0.3
	Yield stress		100 MPa
	Work hardening coefficient		13.1 GPa
Coating material	Material	Active material	Carbon powder (diameter: 5μm, 99.7%)
		Binder	Thermoplastic fluropolymer binder polyvinylidene fluoride (PVDF)
		Solvent	N-Methyl-2-pyrrolidone (NMP)
	Thickness		0.5 mm, 0.7 mm or 1.0 mm
	Young's modulus		0.2 GPa
	Poisson's ratio		0.3

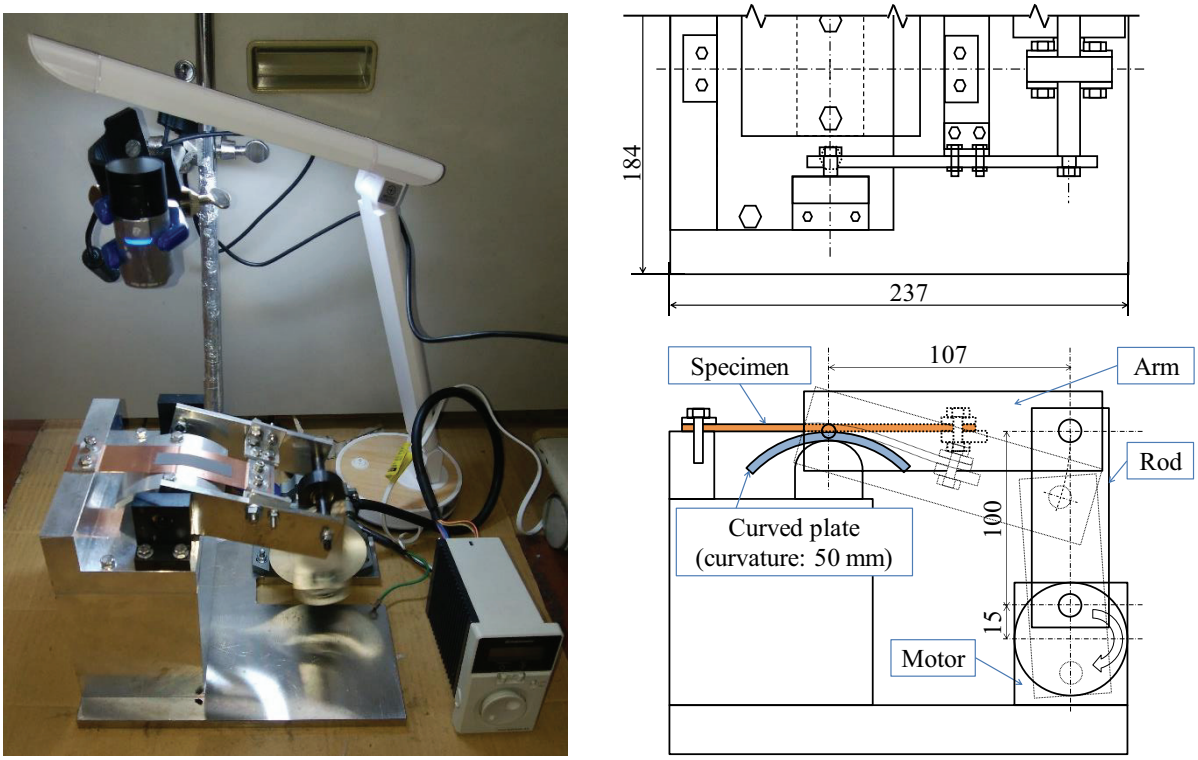

Figure 3: Bending fatigue testing machine

2.3 Finite element simulation

The FE simulation was performed by using the 1/2 FE model as shown in Fig. 4. The 20 nodes hexahedral element was used to construct the FE model. The numbers of the nodes and the elements are 2633 and 368, respectively. The material constants were set as shown in Table 1, and the stress-strain curves are shown as the right of Fig. 4. The quasi-static elastic-plastic deformation analysis was applied, and the deformation behavior of the specimen model under load and after unload was obtained.

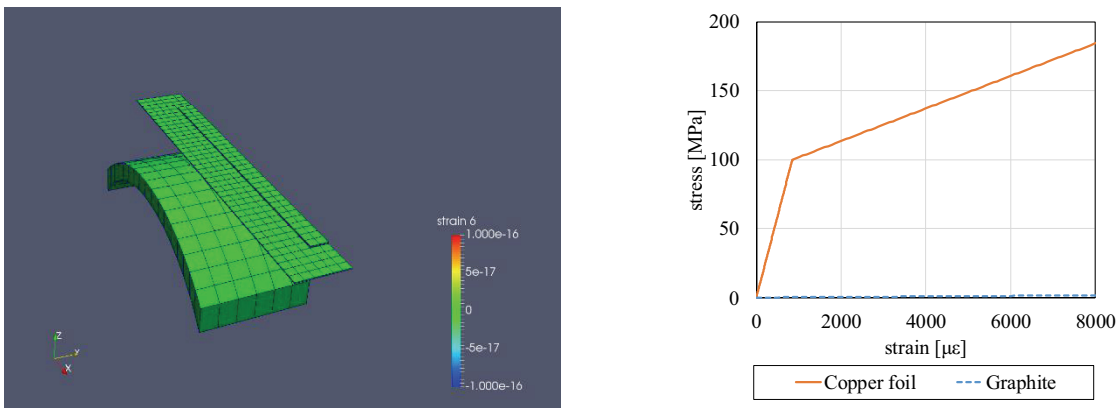

Figure 4: FE model and stress-strain curves

3 RESULTS AND DISCUSSION

3.1 Strain of copper foil

Figure 5 shows the measurement results of the specimen A (copper foil only). Under load, the strain at the point B was not zero in all of the specimens, and it seems that the tension was applied on the specimens. The strain at the point E which was the largest strain was presumed to be the sum of the strains by the bending and the tension. It was assumed that the strain by the tension was equal to the strain at the point B, and the strain by only the bending at the point E was calculated as shown in Fig. 6. The theoretical value of the strain (ε) by the bending can be calculated by the following equation.

$$\varepsilon = t / (2R) \tag{1}$$

where t is the thickness of the specimen, and R is the curvature of the curved plate (50 mm). As shown in Fig. 6, the theoretical values (1000 με and 3000 με) agree with the measured values. Thus, the maximum strain of the specimen applied by the bending fatigue testing

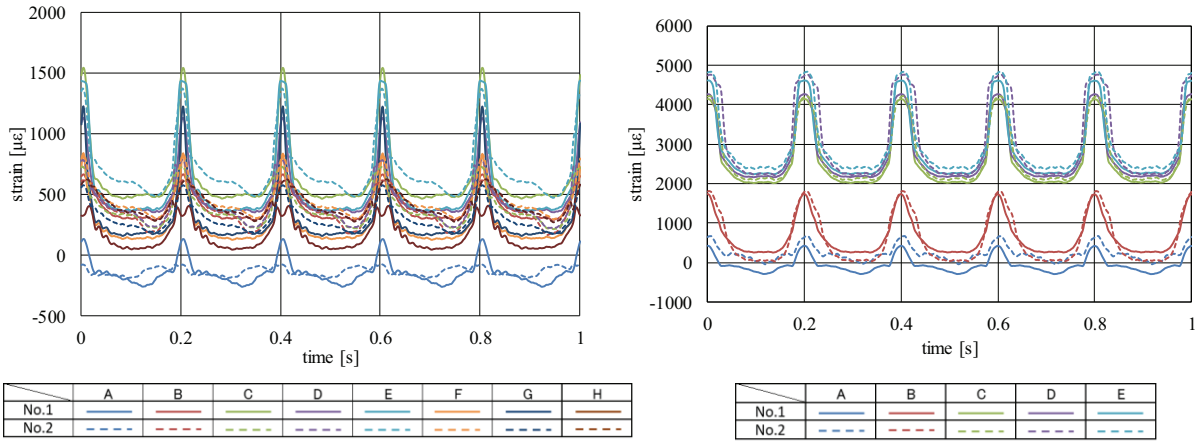

Figure 5: Measured tensile strain of specimen A, thickness: (left) 0.1 mm (right) 0.3 mm

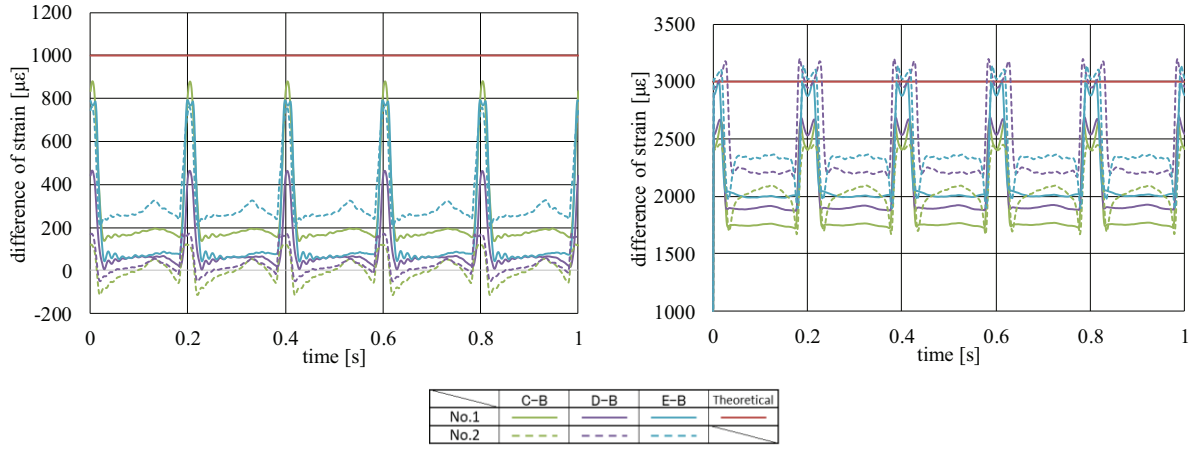

Figure 6: Difference from the measurement point B in tensile strain, thickness: (left) 0.1 mm (right) 0.3 mm

machine is confirmed to be the sum of the strains by the tension and the bending.

After unload, most of the strain was not zero in Fig. 5. The strain was presumed to be the permanent strain. The theoretical value of the permanent strain (ε_p) can be calculated by the following equation.

$$\varepsilon_p = (E \varepsilon_t - \sigma_y) / (E + A) \quad (2)$$

where ε_t is the strain before unload, E is the Young's modulus (118 GPa), σ_y is the Yield stress (100 MPa), and A is the work hardening coefficient (13.1 GPa). According to Eq. (2), the theoretical values of the permanent strain are 587 με (at ε_t = 1500 με) and 3737 με (at ε_t = 5000 με). These values almost agree with the measured strain at the point E after unload as shown in Fig. 5. Therefore, the minimum strain by the bending fatigue testing machine is confirmed to be the permanent strain.

3.2 Fatigue of graphite

Figures 7 and 8 show the examples of the specimen B under the fatigue test. In the fatigue test, the crack initiation was observed at the graphite (coating material) or the copper foil (metallic foil). Regardless of the location of the crack initiation, the crack propagated along the cross direction (the horizontal direction in the figures). The specimen fractured when the crack initiated at the copper foil grew from end to end of the copper foil.

Table 2 shows the summary of the bending fatigue test. When the copper foil was thin, and the graphite was thick, the crack tended to initiate at the graphite. Especially, when the thickness of the graphite was 1 mm, the crack initiated at the graphite by the first bending. The maximum tensile strain was generally applied on the surface by bending, and the strain was proportionate to the square of the thickness according to the theory of elasticity. In addition, the crack initiated on the surface of the graphite, and was Mode I crack (opening

Table 2: Results of bending fatigue test

Test No.	Thickness of copper foil [mm]	Thickness of graphite [mm]	Rotatining speed of motor [Hz]	Number of cycles	Crack initiation
1	0.1	0.7	5	126000	Graphite
2			7	210	Graphite
3				378000	Copper foil
4		1	5	1	Graphite
5				1	Graphite
6			7	1	Graphite
7	0.3	0.5	5	288000	Copper foil
8				288000	Copper foil
9				558000	Copper foil
10				648000	Copper foil
11			7	352800	Copper foil
12			10	486000	Copper foil
13				639000	Copper foil
14		1	5	1	Graphite

mode) as shown in Fig. 7. Thus, the crack initiation depended on the maximum strain by the bending. Similarly, when the copper foil was thick, the crack tended to initiate at the copper foil. Therefore, the location of the crack initiation depended on the thicknesses of the graphite and the copper foil.

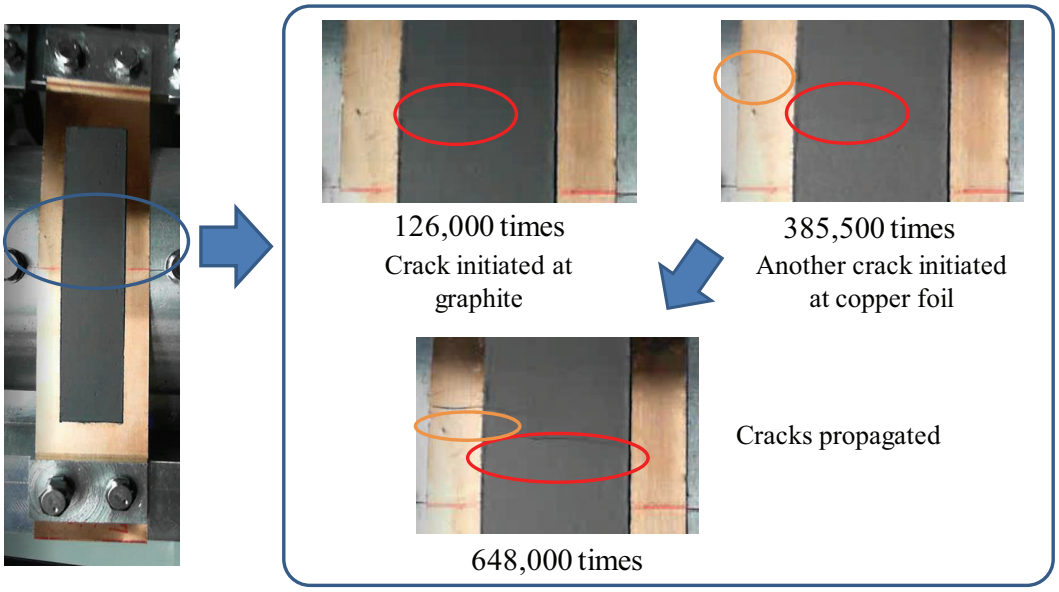

Figure 7: Example of crack initiation at graphite of specimen B, thickness: (copper foil) 0.1 mm, (graphite) 0.7 mm

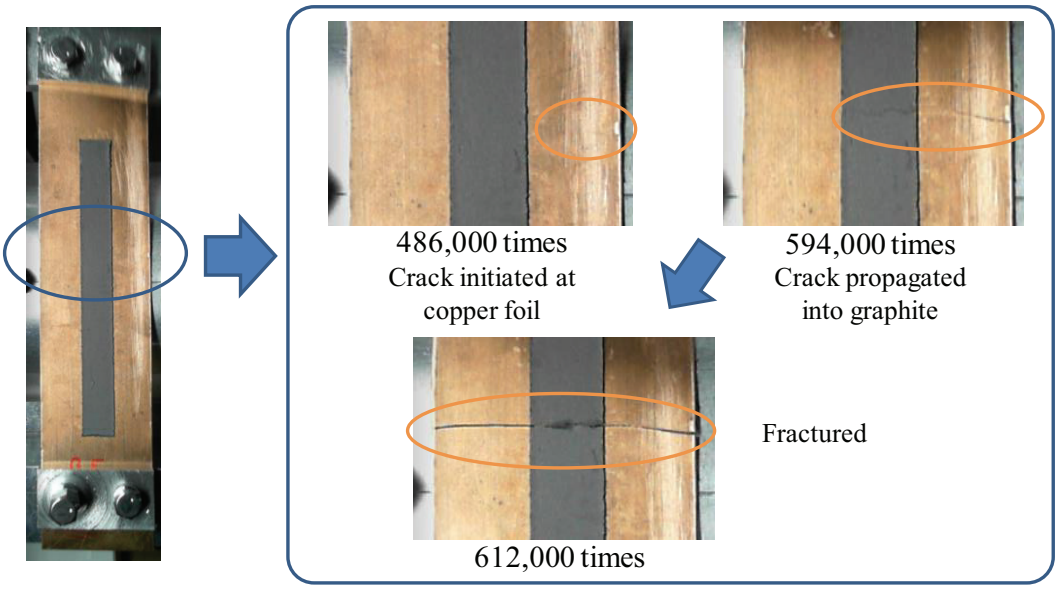

Figure 8: Example of crack initiation at copper foil of specimen B, thickness: (copper foil) 0.3 mm, (graphite) 0.5 mm

3.3 Finite element simulation

Figure 9 shows the example of the FE simulation results. The strain displays the maximum principal strain. Under load, the specimen model was deformed along the surface of the curved plate. The strain was constant at the part contacted to the curved plate. After unload, the permanent deformation was remained similarly to the actual test. Figure 10 shows the strain amplitude in the FE simulation. The horizontal axis means the distance from the center of the specimen model. At the location 10 mm that is the same position as the point E of the specimen A, the strain amplitude is 300 με and 1100 με when the thickness of the copper foil is 0.1 mm and 0.3 mm, respectively. These values agree with the measured values of the specimen A as shown in Fig. 6. Although the strain amplitude in the FE model is larger than that in the actual test at the right side of the point E, it seems that the right side of the point E of the specimen A was not completely contacted to the curved plate in the actual test, and the strain at the right side of the point E was less or equal to the maximum tensile strain. Therefore, it is believed that the mechanical behavior computed by the FE simulation agreed with that in the actual test around the crack initiation part.

The strain amplitude of the graphite in the FE simulation was substituted for the actual value that is difficult to be measured directly. Figure 11 shows the S-N plots of the specimen B. The horizontal axis indicates the number of cycles until the crack initiation in the fatigue test, and the vertical axis is the strain amplitude at 10 mm distance from the center of the FE model of the specimen. Based on Table 2, the S-N plots were discriminated against the

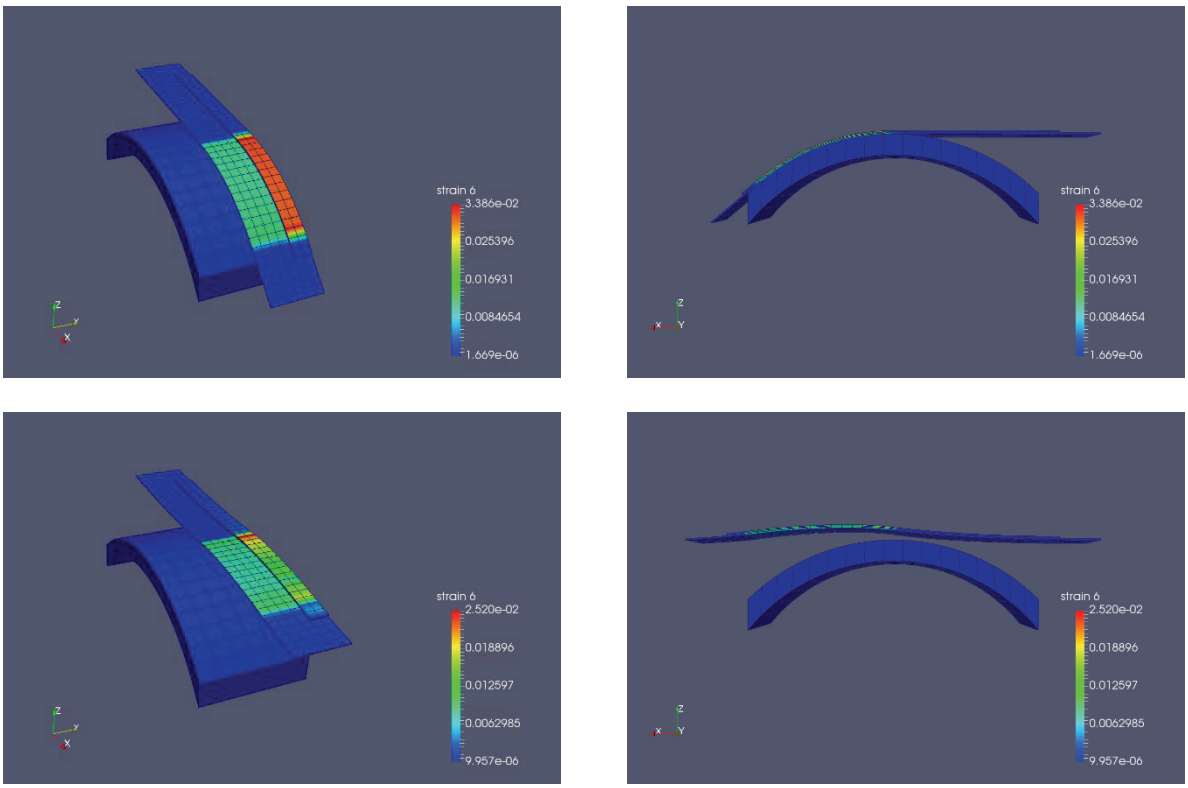

Figure 9: Deformation of FE model, (upper) under load (lower) after unload

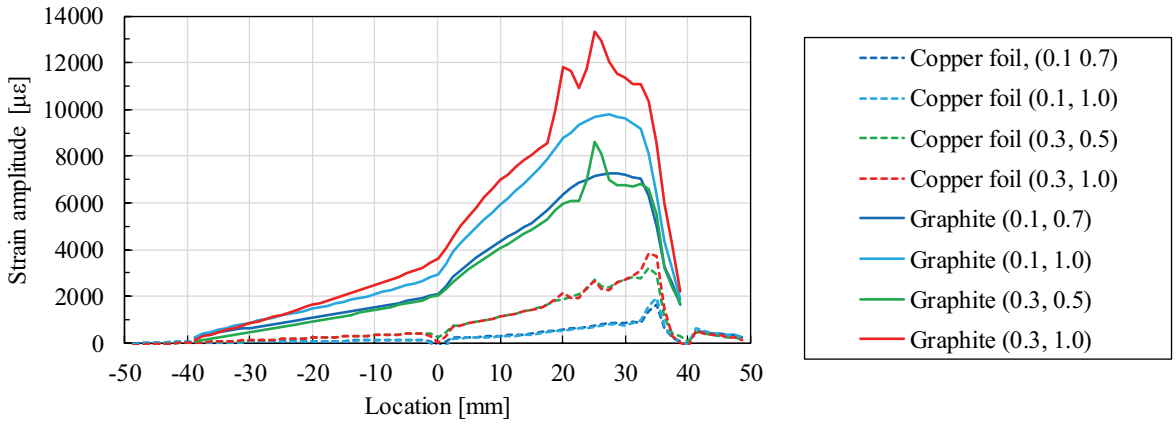

Figure 10: Strain amplitude in FE simulation. (x, y) in the legend means the thickness of the copper foil (x [mm]) and the thickness of the graphite (y [mm]).

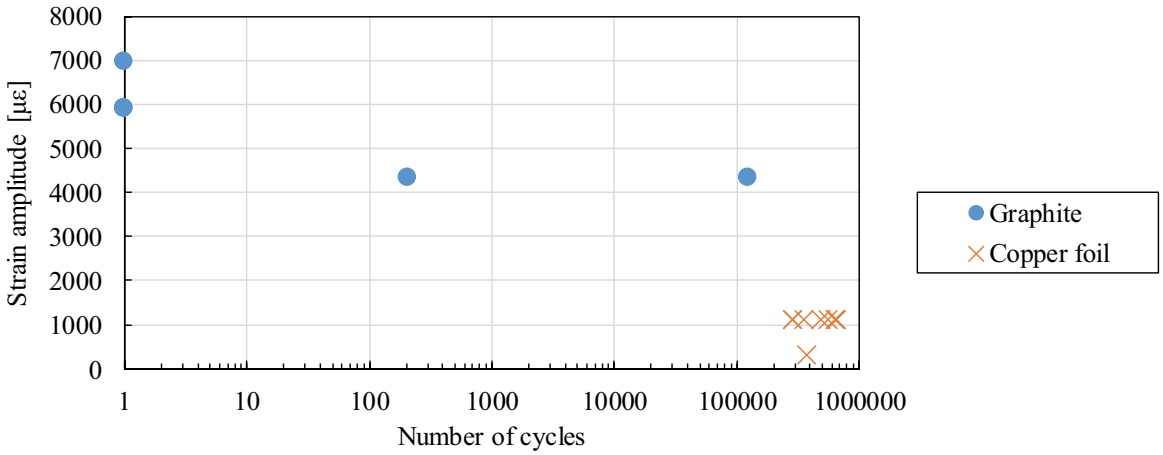

Figure 11: S-N plots

condition of the crack initiation. As shown in Fig. 11, the strain amplitude of the graphite monotonically decreased against the number of cycles until the crack initiation. The S-N plots of the copper foil are located at 1000 με and 300000 to 700000 cycles. These values agree with the fatigue life of the copper C1100 because the number of cycles is 800000 at the stress amplitude 145 MPa (equal to the strain amplitude is 1229 με) according to the reference [11].

4 CONCLUSIONS

The bending fatigue test and the FE simulation were performed by using the anode sheet of the LIB. The location of the crack initiation depended on the thicknesses of the graphite (coating material) and the copper foil (metallic foil). At the first bending, the plastic deformation occurred in the copper foil. The strain amplitude of the graphite monotonically decreased against the number of cycles until the crack initiation. This work was supported by JSPS KAKENHI Grant Number JP16K05989.

REFERENCES

[1] Yang, C., Shao, R., Mi, Y., Shen, L., Zhao, B., Wang, Q., Wu, K., Lui, W., Gao, P. and Zhou, H., Stable interstitial layer to alleviate fatigue fracture of high nickel cathode for lithium-ion batteries, *Journal of Power Sources* (2018) **376**:200-206.

[2] Sahraei, E., Hill, R. and Wierzbicki, T., Calibration and finite element simulation of pouch lithium-ion batteries for mechanical integrity, *Journal of Power Sources* (2012) **201**:307-321.

[3] Greve, L. and Fehrenbach, C., Mechanical testing and macro-mechanical finite element simulation of the deformation, fracture, and short circuit initiation of cylindrical Lithium ion battery cells, *Journal of Power Sources* (2012) **214**:377-385.

[4] Sahraei, E., Campbell, J. and Wierzbicki, T., Modeling and short circuit detection of 18650 Li-ion cells under mechanical abuse conditions, *Journal of Power Sources* (2012) **220**:360-372.

[5] Wierzbicki, T. and Sahraei, E., Homogenized mechanical properties for the jellyroll of cylindrical Lithium-ion cells, *Journal of Power Sources* (2013) **241**:467-476.

[6] Ali, M. Y., Lai, W. and Pan, J., Computational models for simulations of lithium-ion battery cells under constrained compression tests, *Journal of Power Sources* (2013) **242**:325-340.

[7] Lai, W., Ali, M. Y. and Pan, J., Mechanical behavior of representative volume elements of lithium-ion battery modules under various loading conditions, *Journal of Power Sources* (2014) **248**:789-808.

[8] Xia, Y., Wierzbicki, T., Sahraei, E. and Zhang, X., Damage of cells and battery packs due to ground impact, *Journal of Power Sources* (2014) **267**:78-97.

[9] Salvadori, A., Bosco, E. and Grazioli, D., A computational homogenization approach for Li-ion battery cells: Part1 – formulation, *Journal of the Mechanics and Physics of Solids* (2014) **65**:114-137.

[10] Haselrieder, W., Westphal, B., Bockholt, H., Diener, A., Hoft, S. and Kwade, A., Measuring the coating adhesion strength of electrodes for lithium-ion batteries, *International Journal of Adhesion & Adhesives* (2015) **60**:1-8.

[11] Wang, X. G., Crupi, V., Jiang, C., Feng, E. S., Guglielmino, E. and Wang, C. S., Energy-based approach for fatigue life prediction of pure copper, *International Journal of Fatigue* (2017) **104**:243-250.